JEE Journal of Ecological Engineering

Journal of Ecological Engineering 2024, 25(7), 115–136
https://doi.org/10.12911/22998993/188101
ISSN 2299–8993, License CC-BY 4.0

Received: 2024.04.15
Accepted: 2024.05.15
Published: 2024.06.01

Study of Biological Media Interactions in Contact with Cement Paste – An Empirical Analysis

Michał Pyzalski[1]

[1] Faculty of Materials Science and Ceramics, AGH University of Krakow, Al. Mickiewicza 30, 30-059 Krakow, Poland
E-mail: michal.pyzalski@agh.edu.pl

ABSTRACT

The experimental research focused on the influence of solutions containing chicken manure, pig slurry, and silage on the hydration processes of cements and clinker minerals such as C_3S, β-C_2S, C_3A, and C_4AF. The results showed that the hydration of C_3S and β-C_2S led to the formation of various phases, including $Ca(OH)_2$, $CaCO_3$, and various types of poorly crystalline C-S-H phases contaminated with Mg, S, P, Ti, K, and Cl elements. The C_3A phase was the most susceptible to biological corrosion, while the C_4AF phase was the most resistant. Studies on model cement demonstrated a significant influence of solution pH on bacterial presence, where pH ≥ 9 prevented their occurrence, while pH ≤ 4 and pH 6-7 favored their presence. The addition of γ-C_2S and $C_{12}A_7$ phases to the model cement caused a modification of the sample's microstructure and revealed exceptional density, where all spaces were fully occupied by hydration products. Such a model of cement matrix construction prevents and limits the penetration of the corrosive agent into the sample interior. The obtained research results suggest the possibility of using such cement for bioreactor construction and employing additions of calcium aluminates and calcium ferrites to further enhance cement resistance to biological corrosion.

Keywords: biological corrosion, special binders, eco-energy, environmental engineering, anaerobic fermentation.

INTRODUCTION

The degradation of organic matter by microorganisms in oxygen-deprived environments is referred to as anaerobic fermentation. As a result of this process, the primary products are gases in the form of methane and carbon dioxide. An accompanying byproduct of this process is a liquid, contributing to the obtained eco-energy, while the residue contains a solid phase predominantly composed of biodegradation-resistant organic matter, notably lignin from plant waste. These liquid and solid phases serve as valuable fertilizers, enriched with nitrogen compounds, thereby enhancing revenue streams. Anaerobic fermentation plays a crucial role in the effective management of bio-waste, reducing the volume of waste generated by the agricultural, food, and livestock sectors. The resultant biogas can be utilized for heat generation or electricity production. A prevalent method for harnessing energy from biogas is cogeneration, combining heat and power production by utilizing heat from combustion to generate electricity [Fehrenbach et al., 2008, Cole, 1988].Anaerobic fermentation contributes significantly to reducing greenhouse gas emissions, leading to increased profits for biogas plant operators. This sustainable energy production technique is recognized as one of the most efficient and environmentally friendly solutions in the energy sector. Given its myriad advantages, biogas production via anaerobic fermentation is actively encouraged by European Union policies and should be expanded globally, particularly in utilizing diverse organic waste sources for eco-energy production [Evans et al., 2003, Kothari et al., 2014].

Biogas represents the final product of four consecutive chemical reactions in the anaerobic fermentation process: hydrolysis, acidogenesis, acetogenesis, and methanogenesis. Methane fermentation occurs under mesophilic conditions,

ideally at approximately 35 °C, minimizing energy consumption for heating. During the initial hydrolysis stage, complex organic polymers like proteins, lipids, and carbohydrates are broken down into simpler soluble molecules such as amino acids, long-chain fatty acids, and sugars. Subsequently, during acidogenesis, these compounds are further reduced to short-chain volatile fatty acids [Gerardi, 2003, Kayhanian,1999, Li et al., 2011]. Acetogenic bacteria convert organic acids to acetate, hydrogen, and carbon dioxide, which are then metabolized by methanogenic archaea to produce methane and additional carbon dioxide. Under optimal pH conditions for anaerobic fermentation, nitrogen compounds like proteins and urea undergo degradation, leading to the formation of ammonia, primarily as ammonium ions in solution [Bertron, 2014; Bertron et al., 2017; Voegel et al., 2016].

Concrete is of utmost importance in the construction of biogas plants, agricultural, and agro-industrial structures. Its selection is based not only on cost-effectiveness and ease of construction but also on satisfactory air and water tightness, as well as good thermal insulation. Concrete fermentation reactors come into direct contact with the liquid and gas phases of fermenting bio-waste. Due to its chemical properties, this contact can lead to concrete corrosion. Concrete exposed to bio-waste at various stages of anaerobic fermentation may suffer damage due to both chemical and biological factors [Koenig et al. 2016; Bertron et. al., 2013; Koenig et al., 2017].

Chemicals encountered by concrete during anaerobic fermentation include volatile fatty acids released by acidogenic bacteria, ammonia, and dissolved carbon dioxide. These volatile fatty acids, being water-soluble calcium salts, gradually degrade initial hydration products in the cement paste due to their buffering effect and solubility of organic salts [Escadeillas, 2013; Escadeillas, et al., 2008; Carde et al., 1997; Lea, 1965].

Ammonium ions may react with the cement matrix, leading to portlandite dissolution and potential dehydration of CSH phases present in the cement paste matrix. Additionally, carbonation of the cement paste occurs in the presence of carbon dioxide during methanogenic fermentation, altering the pH of the hydration reaction environment. This can lead to the dissolution and recrystallization of portlandite and CSH phases into calcium carbonate. While local carbonation processes may benefit concrete by reducing porosity, in systems exposed to fermentative fluids, bacteria may dissolve calcium compounds, including crystalline carbonates [Baroghel-Bouny et al., 2008; Morandeau et al., 2014; Thiery, 2005].

Microorganisms can accumulate on material surfaces, causing localized high concentrations of aggressive factors, thereby accelerating degradation. Consequently, concrete undergoes gradual deterioration, leading to increased porosity and a heightened risk of reinforcement corrosion. Failure to implement adequate preventive measures can result in concrete structure damage, incurring significant costs and negative environmental impacts, particularly in the case of bioreactor damage [Voegel et al., 2019; Magniont et al., 2011].

EXPERIMENTAL

The research topic encompasses the analysis of the impact of biological factors on the physicochemical properties of cementitious binders and individual synthetic clinker phases, as well as their hydration products. The main goal of these studies was to develop a concept of a new, innovative special binder for use in environmental engineering. Achieving this goal relied on conducting research on synthetic clinker phases and creating conceptual models of special binders.

The experimental research primarily focused on assessing the influence of biological corrosion on cementitious pastes. The next stage involved developing an optimal composition of special binders, from the perspective of environmental engineering, which could be used in the construction of reactors in biogas plants.

The study can be distinguished into two main research areas. The first encompasses the preliminary analysis of commercially available general-purpose cements, which were exposed to biological solutions. The second area focuses on developing a model cement that enables estimation of which component of general-purpose cement is responsible for the occurrence and formation of biological corrosion products, potentially leading to the disintegration of the cement matrix. Addressing this scientific problem involves developing a modern special binder whose phase composition can be adjusted to specific biological exposure conditions. By eliminating or reducing the most susceptible elements to biological corrosion in the binder's phase composition, it will be

possible to obtain a material resistant to biological factors' effects.

Materials

Cement

For the experiment, samples of seven Ordinary Portland Cements (OPC) type CEM I were selected initially. The chemical composition of the Portland cements utilized in the investigation is outlined in Table 1. As a reference (control) medium for exposing the pastes, water with a specified chemical composition (pH = 7.3), detailed in Table 2, was employed.

Biological aggression medium utilized was swine slurry (Tuszyn, Poland) (pH = 4.6), obtained from industrial pig farming. The chemical composition of the aqueous solution derived from biological effluents is provided in Table 3. The studied types of cement consisted predominantly of approximately 95% clinker, along with approximately 5% $CaSO_4 \cdot 2H_2O$ utilized as a regulator for setting time.

During the experiments, types of cement with no additional components such as fly ash, blast furnace slag, zeolite, or powdered calcium carbonate, which have the potential to significantly impact the corrosion process, were utilized. All types of cement employed in the study were of identical strength class, namely 42.5 (this translates into standard mortar reaching a strength of 42.5 MPa after 28 days of hardening.). The cement under examination demonstrated strong initial strength, referred to as R (larger than 20 MPa after 2 days). There was an exception for cement sourced from cement plants in Chełm and Ożarów, designated with the letter N indicating normal initial strength (larger than 10 MPa in 2 days).

Comprehensive details concerning the characteristics of the cement pastes utilized within this study are outlined in the PN-EN-196-1 standard. Rectangular prism samples measuring 4 cm × 4 cm × 16 cm were fabricated for mechanical strength, XRD, thermal, and FT-IR measurements, following the guidelines of standard PN-EN 196-1:2016-07 [PN-EN 196-1:2016-07, 2018]. In accordance with the standard, a water-to-cement ratio of 0.5 was maintained for preparing the cement pastes. The molds containing the cement pastes were left undisturbed for 24 hours

Table 2. Content of selected components in water used for testing the cement paste samples [Durczak et al., 2019]

Parameter	Value [mg/l]
Arsen	< 0.001
Nitrates	1.60 ± 0.03
Cyanides	< 0.005
Fluorides	0.41 ± 0.01
Magnesium	14.00 ± 0.11
Copper	< 0.003
Lead	< 0.001
Mercury	< 0.0001
Sulfate	175.0 ± 12.1
Total hardness $CaCO_3$	377.0 ± 18.6
Calcium	87.0 ± 1.9
Iron	0.20 ± 0.01
Total trihalomethanes (THM)	3.0 ± 0.5
Total chlorates and chlorites	0.100 ± 0.006

Table 1. The chemical compounds in examined Portland cements with sample symbol along with the location of cement origin and the number assigned to all tests performed using cements. [Durczak et al., 2019]

Symbol / Oxide [%]	1	2	3	4	5	6	7
SiO_2	21.70	20.81	21.66	21.56	19.36	22.47	24.27
Al_2O_3	3.30	4.69	5.14	4.76	5.75	6.05	4.29
Fe_2O_3	4.56	3.77	2.77	3.14	2.83	2.72	2.80
CaO	65.52	65.79	65.36	64.94	66.99	63.67	64.01
MgO	1.12	1.33	1.46	1.92	1.68	1.91	1.10
SO_3	3.14	2.65	2.52	2.63	2.20	2.12	2.30
K_2O	0.41	0.77	0.86	0.71	1.05	0.80	1.10
Na_2O	0.20	0.14	0.15	0.30	0.11	0.20	0.10
Cl^-	0.05	0.05	0.08	0.04	0.03	0.06	0.03
Total	100.0	100.0	100.0	100.0	100.0	100.0	100.0

to attain initial strength and preserve the desired beam shapes. After extraction from the molds, the samples underwent an additional 24 – hour curing period in a control-climate chamber under humidity of 100% (relative). Subsequently, the trial specimens were immersed in air-tight containers containing the biological substance, serving as the aggressive medium. Parallel samples were immersed in water to serve as controls. Following a 12 – hour vacuum drying process, the samples were ground using a vibratory mill until a granulation was suitable for sieving through a 0.1 mm sieve. Powdered measurement samples were vacuum-dried for only 1 hour before experiments.

Synthesis of clinker phases

To produce the clinker phases alite – $3CaO{\cdot}SiO_2$, belite – $2CaO{\cdot}SiO_2$, tricalcium aluminate – $3CaO{\cdot}Al_2O_3$, brownmillerite – $4CaO{\cdot}Al_2O_3{\cdot}Fe_2O_3$, and mayenite – $12CaO{\cdot}7Al_2O_3$, we utilized high-purity (99.9%) analytical grade reagents, namely calcium carbonate, aluminum oxide, silicon dioxide, and iron (III) oxide. The raw materials were prepared through homogenization and blending of the weighted portions (ranging from 1–2 kg, based on stoichiometric proportions outlined in subsequent research) in a Deval drum (rotating at 40 rpm) for a duration of 36 hours, followed by drying at 110 °C for 24 hours. The prepared components were securely enclosed in 10 – liter plastic containers for subsequent procedures. Samples of each ingredient were subjected to thermal treatment at 1300 °C for 4 hours to assess losses during roasting. The roasting losses were recorded as follows: 43.73% for $CaCO_3$, 1.94% for Al_2O_3, 0.82% for SiO_2, and 2.34% for Fe_2O_3. Table 4 provides the molar masses of clinker phases along with the synthesis temperature. Weighed appropriate amounts of individual components, in the corresponding stoichiometric portions, were placed in 2 – liter containers. The homogenization process was carried out for 72 hours. The sintering of the samples took place at temperatures provided in

Table 3. Content of chemical components in pig slurry diluted in water [Durczak et al., 2019]

Parameter	Standard	Value [mg/l]
Kjeldahl total nitrogen	PN-EN 25663:2001	1240.0 ± 60.4
Ammonium nitrogen	PN-ISO 5664:2002	1050.0 ± 51.1
Total nitrogen	PN-73/C-04576/14	1350.0 ± 63.5
Nitrite nitrogen	PN-EN 26777:1999	0.032 ± 0.003
Nitrate nitrogen	PN-82/C-04576/08	0.31 ± 0.05
Chrome	PN-EN 1233:2000	0.40 (-)*
Cadmium	PN-ISO 8288:2002	0.05 ± 0.01
Nickel	PN-ISO 8288:2002, PN-EN 13346:2002	0.09 ± 0.01
Lead	PN-ISO 8288:2002	< 0.5
Mercury	EN 13346:2002	< 0.003
Calcium	PN-ISO 6058:1999	68 (-)*
Magnesium	PN-C-04554-4:1999	4.37 ± 0.87
Total phosphorous	PN-EN ISO 6878:2006	352 (-)
Potassium	US EPA 200, 7, ISO 11885	684.0 ± 15.4
Dry mass	CSN ISO 11465	1.31 ± 0.06

Table 4. The chemical composition of cement clinker phases expressed in wt% and the temperature of synthesis of the obtained clinker phases

Phase	CaO	SiO_2	Al_2O_3	Fe_2O_3	Synthesis temp. [°C]
C_3S	73.69	26.31	-	-	1500
C_2S	65.12	34.88	-	-	1450
C_3A	62.264	-	37.736	-	1513
C_4AF	46.16	-	20.98	32.86	1360
$C_{12}A_7$	48.53	-	51.47	-	1320

the tables for a minimum of 5 hours. After taking the samples out from the furnace, the resulting sintered material was subjected to another homogenisation by grinding in an agate to a grain size corresponding to a sieve mesh size of 0.1 mm (agate mill). X-ray analysis on such prepared powder was executed to assure the purity and presence of the obtained sintered material. The synthesis process was repeated until achieving complete phase synthesis.

Preparation of clinker and cementitious samples for hydration studies

5 g weighted samples were compressed in a hydraulic press (PR-25R type, Metimex, Pyskowice, Poland) with a 15 mm matrix diameter at a pressure of 1 bar to form cylindrical shapes (height 6 mm). The prepared samples were then submerged in liquid environments composed of biological substances media with temperatures ranging from 10 to 20 °C. As active media in the biocorrosion process, pig slurry (Tuszyn farm, Poland) (pH = 4.6) obtained from industrial pig fattening, silage made from corn (Smolice farm, Poland) (pH = 6.8), and chicken manure (Woźniak - Fermy Drobiu, Sp. z o. o., Rawicz, Poland) (pH = 6.4) were used. The above-described biological media, weighting c.a. 10 kg, were diluted in 10 litres of distilled water. These prepared aqueous solutions were allowed to mature for a period of 14 days in a tightly closed plastic barrel. Compressed samples of clinker and model cement weighing 5 g were placed in sealed containers filled with water (control sample – W) or corrosive media such as aqueous solutions of pig slurry (G), corn silage (K), and chicken manure (P), and subjected to hydration processes. Synthetic clinker phases were numbered as follows: 1-C_3S+β-C_2S; 2-C_4AF. Model cements were marked as follows: 6 – model cement 8 – model cement with the addition of γ-C_2S and $C_{12}A_7$. A reference (control) was made using a sample exposed to tap water. The samples were kept in water or in a biological corrosion environment at a temperature of 10–20 °C for 10 months. After this period, unbound water was removed from samples using a vacuum pump [10^{-3} Tr] for 1 hour prior to further examination.

Methods

X-ray diffraction

The X-ray diffraction (XRD) method was applied to assess the samples' phase composition. A stabilizing power supply for the X-ray tube PW 1140/00/60 and a vertical goniometer PW 1050/50 (Philips Res., Eindhoven, Netherlands) was provided. The device was equipped with a vertical X-ray apparatus from Philips, with a Cu anode tube (λ = 1.54178 Å). During the measurements, the Ni filter was used. The XRD apparatus was equipped with a PW 2216/20 "fine-focus" X-ray tube with a power of 1.2 kW (the applied tube power was 1 kW, corresponding to a 40 kV tube voltage and a 25 mA cathode filament current). Adjustment of the diffractometer settings allowed for the narrow beam of radiation, improving the precision of data.

Thermal analysis

DTA-TG thermal analysis method with EGA gas analysis was used for samples' thermal characteristics combined with STA 449F3 Jupiter instrument (Netzsch, Krakow, Poland) coupled with the QMS 403 C Aëolos quadrupole mass spectrometer (Netzsch, Krakow, Poland). Measurements were performed on samples weighing approximately 75 mg, on aluminum oxide (Al_2O_3). During the experiment, a flow rate of 40 ml/min and a heating rate of 15 °C/min synthetic air atmosphere was provided. The measurements were obtained in the temperature range from 30 °C to 1000 °C. Based on the TGA mass loss measurements in characteristic temperature ranges, the content of individual components in the tested samples was estimated. The $Ca(OH)_2$ and $CaCO_3$ content in the original samples were calculated from TG curves using the below formula:

$$X = \Delta M_{TG} \times S \quad (1)$$

where: X – % (m/m) content of the component in the sample, ΔM_{TG} – the mass loss based on the *TG* curve in the temperature range characteristic for a given component, expressed in % (m/m), S – stoichiometric coefficient resulting from the chemical composition of a given component. S value of 4.12 was used to calculate the content of $Ca(OH)_2$ while the content of $CaCO_3$ was assessed using S = 2.2.

FT-IR measurements

Fourier-transform infrared (FT-IR) spectroscopy was utilized to determine the samples' transformation upon storage in biological media. The structure of cementitious paste during storage in liquid pig slurry for 10 months was examined using a Nicolet iS50 FTIR spectrometer (Thermo Scientific, Madison, WI, USA) with an attenuated total reflectance (ATR) diamond accessory (GladiATR attachment, PIKE Technologies, Madison, WI, USA). Spectra in the range between 4000 cm^{-1} and 500 cm^{-1}, with a 4 cm^{-1} nominal resolution were collected. Sixty-four scans were collected in the "atmospheric correction" mode. Baseline correction was executed with OMNIC software (version 8.2, Thermo Fischer Scientific Inc., Madison, WI, USA). Three documented collections of spectra were averaged. Spectral analysis was conducted using the GRAMS AI Spectral Notebase (Thermo Fisher Scientific, Madison, WI, USA). Plots were drawn with Grapher 4 software (Golden Software, LLC, Golden, CO, USA).

The compressive strength tests

After 10 months of conditioning in H_2O (reference) or an aqueous solution of pig slurry tests of the mechanical strength were done on rectangular prism-shaped cement blocks with dimensions of 40 mm x 40 mm x 160 mm. Samples used as controls were labelled from 1_1 to 7_1 (water), while samples subjected to pig slurry were labelled from 1_3 to 7_3 (pig slurry).

RESULTS

Research on the interaction of biological media with cementitious binders

The study presented the results of phase composition analysis (Fig. 1) and demonstrated that besides the presence of characteristic diffraction peaks indicating the presence of crystalline phases, the elevated background in the range of 25–40 degrees 2Θ indicates the presence of a non-crystalline (amorphous) phase. The elevation of the diffraction background may also be caused by the increasing content of pseudo-crystalline hydrated calcium silicates (C-S-H); however, the influence of living matter on the overall XRD patterns cannot be excluded. The diffraction peaks that are first noticeable originate from the crystalline portlandite $Ca(OH)_2$ and calcite $CaCO_3$, and occur in both reference samples and samples subjected to biological degradation. However, based on the conditions of the surrounding environment of the cementitious binders, distinct changes in the relative intensities of reflections from these phases are also observed in the XRD patterns, confirming the variable mass portlandite/calcite fraction ratio. In samples taken out from pig slurry, an apparent reflection intensity decrease of peaks attributed to the portlandite phase is observed. Additionally, an accompanying increase in the intensity of peaks characteristic of calcite is noticed. These trends in intensity changes indicate an interaction (reaction) between calcium hydroxide and carbon dioxide, produced by bacteria during oxygen-deprived (anaerobic) respiration. The visible higher background level on the diffraction patterns in samples exposed to biological suspension conditions shows a slight flattening in the range of reflection angles 25–40 2Θ. This can be associated with the process of progressive corrosion, during which the breakdown of the C-S-H phase occurs, creating ettringite in environments with surplus carbonate ions and decreased temperatures of reaction. This was also confirmed in all ettringite-containing samples subjected to biological corrosion. Additionally to C-S-H phase - a hydration product of calcium silicate, the presence of unreacted crystalline phases such as tricalcium aluminate and dihydrate gypsum is observed. In all tested samples, the presence of unreacted β-C_2S clinker phase, undergoing slow hydration, was also confirmed.

The comparison of all tested binders revealed slight but significant phase composition differences between the tested samples. In addition to ettringite, the presence of a secondary phase of ettringite was detected in all samples, which theoretically should not be present in the phase composition of cementitious binders hydrated for 10 months. This phenomenon indicates that the formation of subsequent corrosion products, such as ettringite, is possible in the later stages. Comparing H_2O – treated samples with samples interacting with living matter, i.e., bacteria, indicates an increase in the concentration of calcium carbonate phase as a product of carbonation during the oxygen-deprived bacterial respiration. The findings of the phase composition analysis of cementitious binders are confirmed by thermal analysis, where all samples showed similar courses of thermal curves. The observed variations pertained to the concentrations of individual components [Sujak

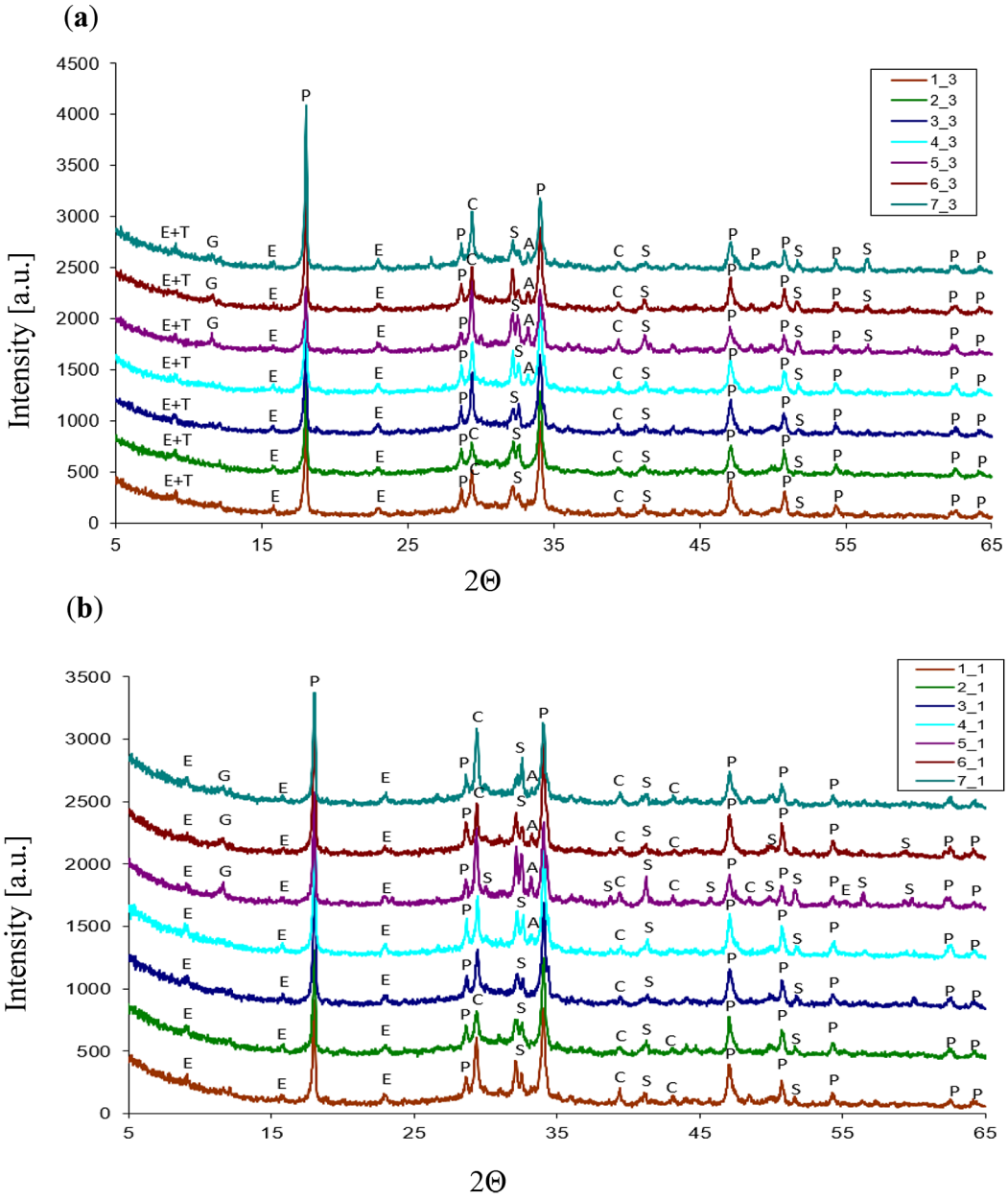

Figure 1. Cement pastes X-ray diffractograms obtained posterior 10 months of exposure to distilled water (panel b, samples from 1_1 to 7_1) and pig slurry (panel a, samples from 1_3 to 7_3); Description of crystal phases: T –$C_3S{\cdot}CO_2{\cdot}SO_3{\cdot}15H_2O$, E–$C_3A{\cdot}3CaSO_4{\cdot}32H_2O$, P –$Ca(OH)_2$, C –$CaCO_3$, S –$C_2S$ and G –$CaSO_4{\cdot}2H_2O$

et al., 2021; Durczak et al., 2021]. Further observations involving comprehensive thermal analysis drew attention to thermal transformations specific to this material type happen across three distinct temperature intervals (Table 5, Table 6). The first of them (from room temperature (RT) to about 300 °C) characterizes the release water not bonding chemically, followed by gypsum, ettringite as well as C-S-H phase dehydration, evident by mass loss on the TG curve, accompanied by an endothermic effect as visible on the DTA curve. The next temperature interval starts from about 450 °C and finishes at about 550 °C. Two phenomena, mass loss on the TG curve and an endothermic effect on the DTA curve indicating processes related to the thermal breakdown of portlandite during dihydroxylation are visible. The abovementioned changes are associated with H_2O release into the atmosphere. The third temperature interval (from about 650 °C to about 1000 °C) coinciding with the mass loss visible on TG curve accompanied by the endothermic effect on the DTA curve is associated with the thermal decomposition of carbonate and resulting with

Table 5. The reduction in mass of the examined samples and the distinctive temperature intervals observed during heating according to the TG curve [Sujak et al., 2021]

Sample	Temperature range [°C]			
	Dehydration	Dehydroxylation	Decarbonatization	
	30 ÷ 360	430 ÷ 580	580 ÷ 695	695 ÷ 1000
1_1	12.64	4.40	0.82	1.96
2_1	13.41	4.21	0.76	0.94
3_1	12.64	4.24	0.83	2.23
4_1	12.90	4.61	0.71	1.76
5_1	11.51	3.36	0.75	2.30
6_1	13.27	4.59	0.75	1.83
7_1	12.44	3.56	0.93	2.50
1_3	13.20	4.41	0.88	2.30
2_3	13.96	4.18	0.83	1.46
3_3	14.09	4.06	0.94	2.75
4_3	12.60	4.49	0.93	2.49
5_3	11.63	3.07	0.99	3.51
6_3	13.71	4.14	1.04	2.94
7_3	13.47	3.42	1.38	2.80

Table 6. The quantitative composition of portlandite – $Ca(OH)_2$ and calcium carbonate $CaCO_3$ [% (m/m)] in the examined cement pastes determined based on the mass reduction (loss) in the respective temperature ranges [Sujak et al., 2021]

Sample	$XCa(OH)_2$	$XCaCO_3$
	% (m/m)	% (m/m)
1_1	18.13	6.31
2_1	17.35	3.86
3_1	17.47	6.95
4_1	18.99	5.61
5_1	13.84	6.92
6_1	18.91	5.86
7_1	14.67	7.79
1_3	18.17	7.22
2_3	17.22	5.20
3_3	16.73	8.38
4_3	18.50	7.76
5_3	12.65	10.22
6_3	17.06	9.03
7_3	14.09	9.49

the CO_2 release. The temperature-induced breakdown of carbonates occurs in the temperature interval between 650 °C and c.a.1000 °C. Two stages can be observed, indicating the presence of two forms of carbonates. The first occurs within the temperature range of 580–695 °C, with a lower mass loss value, and the second in the range of 695–1000 °C. A decrease in the amount of portlandite and an increase in the amount of calcite in samples exposed to pig slurry compared to samples stored in aqueous solutions were demonstrated. The probable cause of this phenomenon is the secondary carbonation of calcium hydroxide by carbon dioxide released during the anaerobic respiration process of bacteria present in pig slurry [Sujak et al., 2021; Durczak et al., 2021].

The above studies were complemented by infrared spectroscopy analysis, performed for each sample in the range of 4000 cm^{-1} to 500 cm^{-1} (Fig. 2). The analyses of cementitious binders exhibited similar spectroscopic profiles. However, detailed analysis revealed visible trends indicating the destruction of the cementitious binder structure depending on the conditions of its exposure. The absorption spectra of cementitious binders stored in water were compared with the spectra of cementitious binders exposed to aqueous suspensions of pig slurry. For most samples, the effects occurring in the absorption range of 1500–1300 cm^{-1}, which can be assigned to the C-O group asymmetric stretching mode characteristic for calcium carbonates ($CaCO_3$), were accompanied by a decrease in maxima in the range of 1100–800 cm^{-1}, characteristic of the primary phase of Portland cement binding – C-S-H. Another spectroscopic region indicating structural damage was found at wavenumbers higher than 3640 cm^{-1}, showing

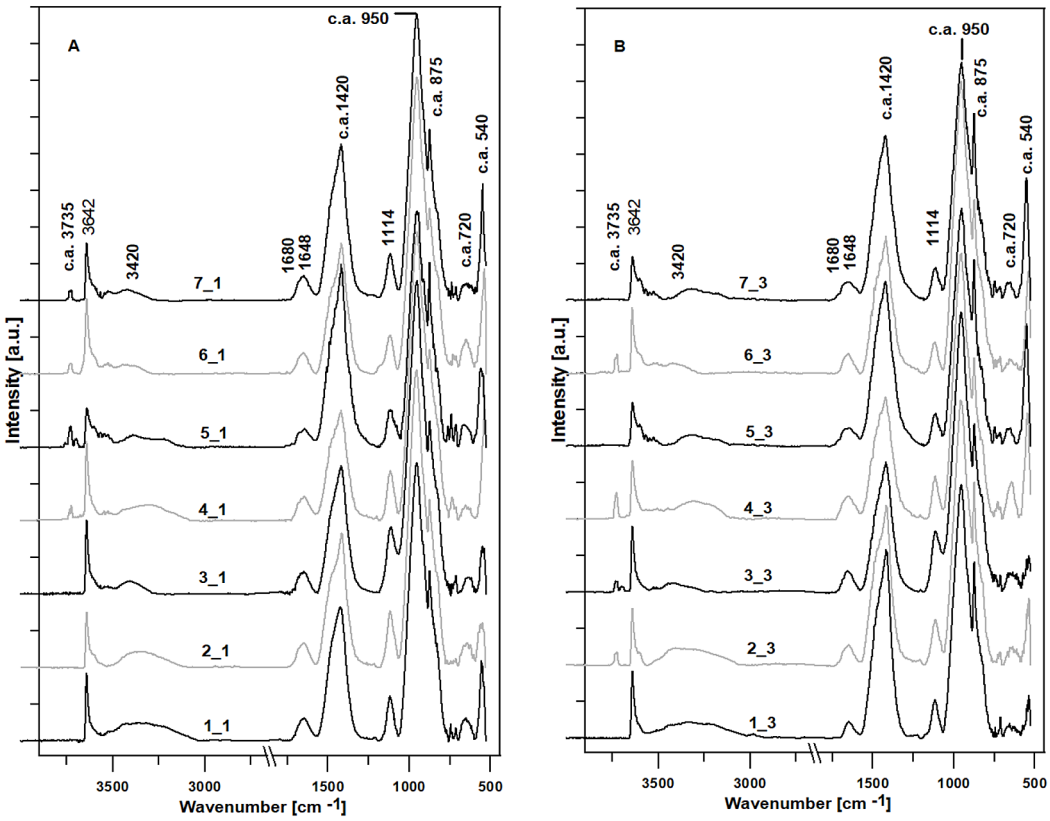

Figure 2. Surface-normalized FT-IR spectra of the examined cement pastes in the range of 4000–500 cm-1. Cement pastes subjected to water (Panel A: references, series 1) and samples kept in a pig slurry for a period of 10 months (Panel B, series 3)

vibrations of surface OH groups and low-intensity vibrations of interlayer H_2O molecules bound by hydrogen bonds [Sujak et al., 2021].

The samples' exposure to pig slurry caused alterations in the O-H groups, likely resulting from the formation or disruption of hydrogen bonds. Studies indicating structural damage found confirmation in the results of compressive strength tests for samples of cementitious binders subjected to compression tests (Fig. 3). Binders stored in water achieved values of 100 MPa or higher. Samples stored under biological corrosion conditions achieved compressive strength values lower by 10 to 16% compared to reference (stored in water). The compressive strength concerning pig slurry-exposed samples ranged from 80 to 99 MPa. The

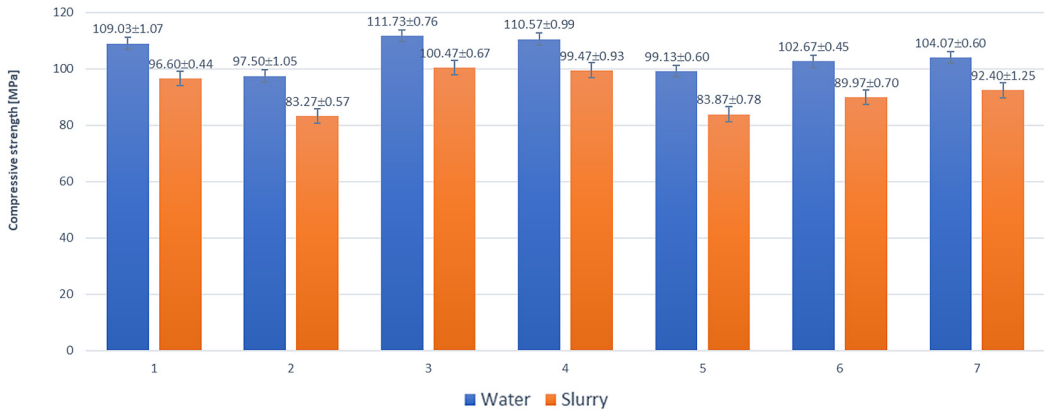

Fig. 3. Mean compressive strength (n = 6) after 10 months [MPa] of cement pastes 1–7 ±S.D. Samples exposed to water (reference) – blue, samples exposed to biological corrosion – orange. X axis – cement pastes (1–7) subjected to compressive strength tests. Y axis – values of compressive strength [MPa]

mechanical strength decrease in samples subjected to biological corrosion was linked to the surface corrosion as a result of biological aggression, leading to a reduction in the cohesion of the cementitious matrix consisting of hydrated calcium silicates (C-S-H). Additionally, in samples seasoned in the corrosion medium, both phase composition thermal studies indicate an increased content of calcium carbonate and secondary ettringite. The formation of calcium carbonate, on one hand, seals the surface of cementitious binder samples, but it can also contribute to a decrease in the strength parameters of the tested samples. One might infer that the presence of exposed pores on the sample surface, where the corrosive medium penetrates deeper, may result in the creation of hydration products that reduce the samples' mechanical characteristics [Pyzalski et al., 2021; Pyzalski et al., 2023].

The research on the impact of biological media on synthetic clinker phases

The results of the research including the degree of reaction of C_3S and βC_2S clinker (symbol 1), as well as the content of newly formed phases

In typical Portland cements, besides alite (C_3S), there is usually belite (β-C_2S) present in amounts ranging from 10 to 25% by weight. The formation of these phases occurs during the high-temperature synthesis process of calcium oxide and silica. It is also known that these phases differ in their activity towards water, and the products of their reaction with water form C-S-H type compounds, characterized by different structure and chemical composition [Sujak et al., 2021; Durczak et al., 2021; Pyzalski et al., 2021; M. Pyzalski et al. 2023].

In the context of the above, it was assumed that to maintain analogy in later hydration processes, preparations of C_3S and C_2S phases would be synthesized together, analogous to classical Portland cements. By properly preparing the raw material set and synthesizing it under high-temperature conditions (1500 °C/5h), the intended goal was achieved, obtaining a preparation with a composition of 75.5% C_3S and 24.5% C_2S. Subsequently, this preparation was crushed and formed into pellets, and subjected to the described research procedures regarding the influence of biological factors and other chemical factors. In the case of clinkers and samples of model cement, the samples were subjected to studies in a water environment (W), pig slurry (G), corn silage (K), and poultry manure (P). The research results are presented in Table 7 and Figure 4 [Sujak et al., 2021; Durczak et al., 2021; Pyzalski et al., 2021; Pyzalski et al. 2023].

Analyzing the results of the degree of reaction of the C_3S and β-C_2S phases, it was found that this degree varies depending on the reaction environment from 56.5% to 73.0% for the C_3S phase and from 47.0% to 18.5% of the mass of the phase for β-C_2S. The observed trends are consistent with the results of studies found in the scientific literature [Sujak et al., 2021; Durczak et al., 2021; Pyzalski et al., 2021; Pyzalski et al. 2023]. It is worth noting that in addition to the hydration reaction in a water environment, there is an increasing tendency in the degree of reaction of the tested phases in the G, K, P preparations for the C3S phase (G > K > P), while for β-C_2S, there is a decreasing tendency (P > K > G).

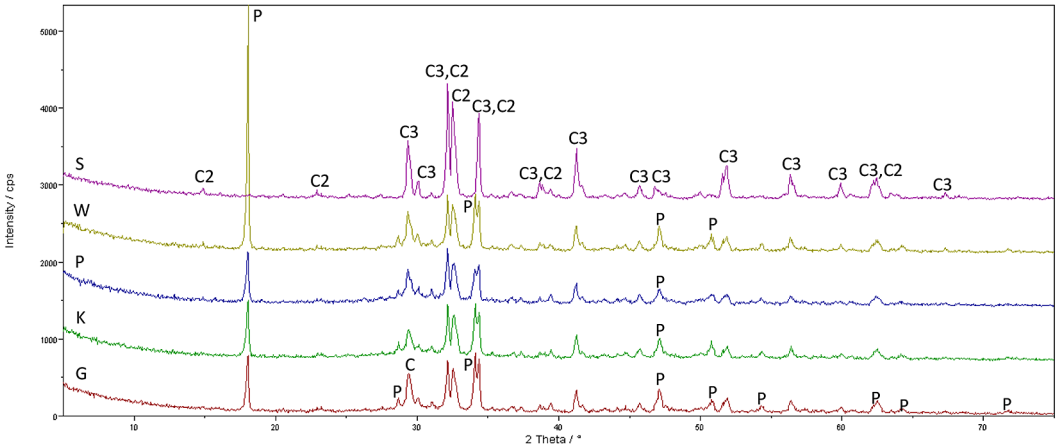

Figure 4. X-ray diffraction pattern of the sample with symbol 1. Sample composition: 75.5% C_3S and 24.5% C_2S%. Description of crystal phases: C2- C_2S; C3- C_3S ; P – $Ca(OH)_2$; C – $CaCO_3$

Table 7. Quantitative analysis of crystalline phases in C_3S and C_2S sample expressed in wt%

Newly formed phases	Content in % by weight phases resulting from reactions with aqueous solutions			
Sample designation	1W	1P	1K	1G
Reaction environment	Water	Chicken litter	Corn silage	Pig slurry
$Ca(OH)_2$	15.0	9.0	11.0	12.5
$CaCO_3$	2.5	11.0	7.0	5.5
Amorphous phases (CSH)	Amorphous phases visible in the background are hydrated calcium silicates, poorly crystalline CSH compounds, contaminated with chemical compounds containing elements such as; K, Na, Al, Fe, P			
	35.5	47.0	44.0	40.5
GOF	4.62	5.41	5.03	4.17
pH	12.81	10.64	10.21	6.87

The same trends were also observed in the assessment of the influence of the pH of the reaction environment (with the exception of results for H_2O), where an increase in the alkalinity of the reaction environment accompanied an increase in the degree of reaction of the C_3S phase, while in the case of the β-C_2S phase, the opposite trend was observed. The only crystalline products, besides the unreacted portions of C_3S and β-C_2S, formed during hydration processes, are portlandite ($Ca(OH)_2$) and calcite ($CaCO_3$). The increase in the amount of crystalline products correlates with the increase in the alkalinity of the solutions, including the content of portlandite $Ca(OH)_2$ (G > K > P; from 13 to 9.5%). At the same time, quantitative results of calcite content in the samples indicate a clear relationship between an increase in pH and the level of calcite content (G > K > P; from 4.5 to 5.5%).

In the analysis of the presence of the amorphous phase, the obtained quantities of its content do not provide grounds for seeking correlations with other results. This is due, on the one hand, to qualitative and quantitative issues linked to the C-S-H phases formation along with concurrently occurring processes of calcite formation resulting from carbonation processes, as well as simultaneous formation of portlandite. CO_2 reaction processes resulting from biochemical reactions may affect the speed and amount of $CaCO_3$ formation. The obtained research results, within the sensitivity of X-ray detection methods, showed that apart from the mentioned hydration products, no other crystalline compounds were found. Considering the fact of high pH values exceeding 9 in samples 1P and 1K, the influence of biocorrosion processes significantly slowed down due to the absence of active biological matter.

Besides the mentioned main crystalline phases $Ca(OH)_2$ and $CaCO_3$, the remaining part of the preparations consists of amorphous C-S-H phases and unreacted remnants of initial phases. Taking into account the need for a somewhat more precise definition of the amorphous phase, the assumptions of Taylor and Diamond were adopted, suggesting that there are four variants of it, namely C-S-H I, C-S-H II, C-S-H III, and C-S-H IV. The first two differ from each other in the molar ratios of C/S. In the C-S-H I phase, this ratio is less than 1.5, whereas in the case of the C-S-H II phase, the ratio C/S > 1.5. Additionally, these variants can be distinguished based on their morphological appearance. The C-S-H I phase occurs in fibrous form, C-S-H II has a reticular structure called "honeycomb," while C-S-H III forms isometric grains, and C-S-H IV forms agglomerates (clusters) recognized under an electron microscope as a dense gel. It should be noted that all types of C-S-H phases are difficult to identify and distinguish solely by X-ray methods because they are usually poorly crystallized, and their presence, in the case of X-ray studies, is effectively revealed by raising the background of the diffraction pattern in the range of angles 15 ÷ 40 2Θ. An additional difficulty in identifying the discussed phases is that in aqueous solutions of poultry manure, silage, and slurry, there are elevated contents of chemical compounds containing elements such as K, Na, Al, Fe, P, and other organic impurities contaminating and modifying the structures of amorphous C-S-H phases. It is worth emphasizing that despite the difficulties, relatively low goodness of fit (GOF) coefficients were obtained in X-ray studies, which provides grounds for assessing the reliability of the presented analysis results. It was also noted that all samples (in pellet form) of the tested preparations removed from their maturation environments retained their original shape and showed no signs of corrosion despite their relatively high hardness. Only depending on the nature of the environment in which they matured, they changed their color.

The results of the research including the degree of reaction of the C_4AF phase (symbol 2), as well as the content of newly formed phases

In traditional Portland cements, alongside alite (C_3S) and belite (β-C_2S), there is typically also the phase C_4AF, whose content varies from about 5 to 25% by weight. This phase belongs to a series of solid solutions starting from C_2F up to the hypothetical "C_2A", occupying a middle position in this series. In Portland clinkers and cements, it is known as brownmillerite. Due to its place in this series, the chemical composition of the C_4AF phase can vary significantly. This compositional diversity has serious consequences for the hydraulic activity of different samples of such compounds. Generally, phases richer in Fe_2O_3 exhibit lower activity towards H_2O, emitting small amounts of heat during the hydration process and showing greater resistance to aggressive environments [Pyzalski et al., 2023; Durczak et al., 2023]. The C_4AF phase was subjected to X-ray radiation analysis, which confirmed the achievement of the intended goal, namely obtaining a preparation corresponding to the parameters of the C_4AF phase, with a small amount of mayenite admixture – $C_{12}A_7$. The analysis of

Table 8. The degree of hydration in the sample with symbol 2 (C_4AF and $C_{12}A_7$) expressed in wt%

Phases	Reaction degrees in %			
Sample designation	2W	2P	2K	2G
Reaction environment	Water	Chicken litter	Corn silage	Pig slurry
C_4AF	29.0	25.5	28.0	31.0
$C_{12}A_7$	100	100	100	100

Table 9. Quantitative analysis of crystalline phases in sample with symbol 2 (C_4AF and $C_{12}A_7$) expressed in wt%

Newly formed phases	Content in % by weight phases resulting from reactions with aqueous solutions			
Sample designation	2W	2P	2K	2G
Reaction environment	Water	Chicken litter	Corn silage	Pig slurry
$Ca(OH)_2$	0	0	0	0
$CaCO_3$	1.5	5.5	6.5	2.0
$C_{3÷4}(Al,Fe)H_{6÷19}$	18.5	3.0	6.0	10.5
Other crystalline phases	Hydroxy-AFm phases, monocarboaluminate $C_4A\hat{C}H_{12}$, hemicarboaluminate $C_4A\hat{C}_{0.5}H_{12}$ and amorphous iron hydroxides visible in the background			
Amorphous phases	16.5	21.5	26.0	20.0
GOF	3.81	5.34	3.94	4.25
pH	12.32	10.86	9.06	7.12

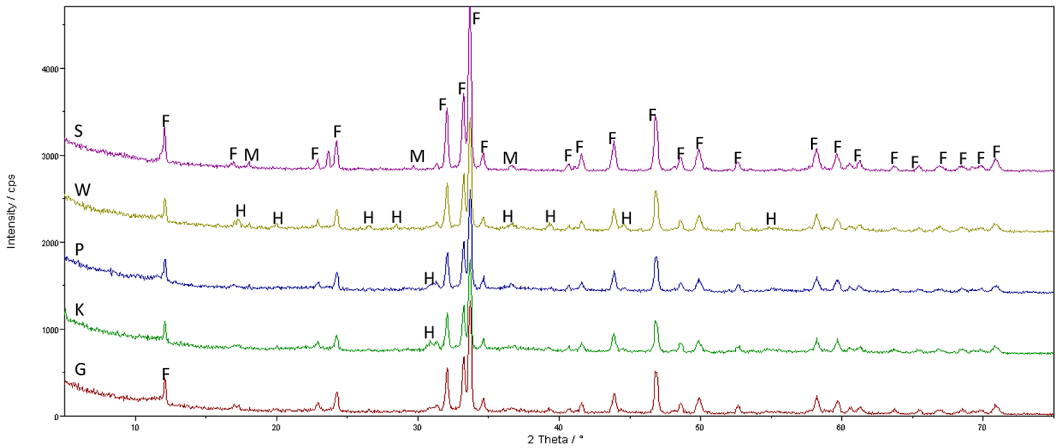

Figure 5. X-ray diffraction pattern of the sample with symbol 2. Sample composition: C_4AF and $C_{12}A_7$. Description of crystal phases: F - ferrite; M - $C_{12}A_7$; H - $C_{3÷4}(Al,Fe)H_{6÷19}$

research results (Tables 8, 9, and Figure 5) suggests that the examined samples contain small amounts of hydration reaction products, consisting of various calcium aluminate hydrates, hydrogarnet-type phases, hydroxyl-AFm (OH-AFm), monocarboaluminate $C_4A\hat{C}H_{12}$ (Mc), hexacarboaluminate $C_4A\hat{C}_{0.5}H_{12}$, as well as amorphous phases of iron and aluminum hydroxides, often contaminated with other elements. Such presence of amorphous phases significantly complicates their unambiguous identification. Analysis of the degree of reaction of the synthetic C_4AF phase in contact with water and aqueous solutions of biological waste confirms the highest resistance of this phase to their action among all mineral components of cements.

Regardless of the pH level, type of reagents, and solutions, the degree of reaction varies within the range of 25% to 31%, leading to a low level of amorphous phase content. This phase includes accessory phases, but visible in the background, such as AFm phases, monocarboaluminate $C_4A\hat{C}H_{12}$, hemicarboaluminate $C_4A\hat{C}_{0.5}H_{12}$, and amorphous iron hydroxides. The presence of amorphous phases was assessed at levels ranging from 15% to 23%. In the case of a small amount of hydration products, equally difficult to identify crystalline hydration products are phases of C4AF compounds resembling compositions of $C_3AH_6 \div C_4AH_{19}$, $C_3FH_6 \div C_4FH_{19}$, or $C_3(A,F)H_6 \div C_4(A,F)H_{19}$, contaminated with other additives. Similar to the hydration processes of calcium silicate phases, elevated contents of chemical compounds containing elements such as K, Na, Al, Fe, P, and other organic impurities contaminating and modifying the structures in the used reaction media (poultry manure, silage, slurry) lead to difficulties in identifying hydrate phases [Pyzalski et al., 2023; Durczak et al., 2023].

It was also noted that all samples in pellet form of the tested preparations, removed from their maturation environments, retained their original shape and showed no signs of corrosion with high hardness. The level of goodness of fit (GOF) coefficients in quantitative X-ray studies ranging from 3.8 to 5.3 indicates the high reliability of the presented research results

Test results of the degree of reaction of the model cement (symbol 6) and the content of newly formed phases

Classical Portland cements mainly contain the following mineral phases: alite (C_3S), belite (β-C_2S), C_3A, and brownmillerite (C_4AF), with the addition of about 4% gypsum. In this study, it was decided to develop a model cement, designated as number 6, based on synthetic and already possessed minerals. It was assumed that the mineral composition of this synthetic cement should approach the following percentage shares of phases: approximately 55% C_3S, approximately 20% β-C_2S, approximately 10% C_3A, approximately 10% C_4AF, and about 5% gypsum. The synthetic minerals, which were owned and crushed, were measured in appropriate weight proportions, then mixed and homogenized for a period of 5 hours. As a result of these actions, a two-kilogram sample of model cement "6" was obtained. Its mineral composition was determined by X-ray methods without using an internal standard and is as follows (wt.%): C_3S – 49.5%; β-C_2S – 24.7%; C_3A – 7.8%; C_4AF – 10.0%; Gypsum – 8.0%. [Pyzalski et al., 2023; Durczak et al., 2023].

From the obtained sample of model cement, pellets were prepared, which were then placed in containers with water and water mixtures with biological additives. After 10 months of curing, the samples were dried, crushed, and subjected to planned examinations. It is widely accepted that the processes occurring during the hydration of individual phases of the model cement significantly differ from the process occurring in the natural mixture, which is industrial Portland cement. After mixing the cement with water, the pH reaches a level above 12.0 in a short time and remains at this level for a longer period. As a result, hydration processes of cement minerals occur under constant pH conditions. However, other factors such as mutual interaction of chemical processes, amount of heat released during hydration, degree of cement grinding, purity and amount of added water, presence of additives, significantly affect the hydration processes.

Changing the environment from water to aqueous solutions with biological additives should influence both qualitatively and quantitatively the course of hydration processes. The results of the conducted research confirm the existence of distinct differences in the degree of reaction, quality and quantity of newly formed hydration products, and in the area of formation of amorphous phases. Analyzing the phase of alite C_3S and belite β-C_2S and their hydration processes, issues regarding the qualitative presence of two crystalline phases: $Ca(OH)_2$ and $CaCO_3$ have already been discussed. In addition to the main crystalline phases, some preparations contain amorphous CSH phases and unreacted parts of starting phases. For precise

identification of the amorphous phase, four varieties are used according to the assumptions of Taylor and Diamond: CSH I, CSH II, CSH III, and CSH IV. Phase CSH I is characterized by a molar ratio of C/S less than 1.5, while phase CSH II has a C/S ratio greater than 1.5. Additionally, SEM methods are used for the identification of these hydrates, allowing them to be distinguished based on morphology. Phase CSH I occurs in a fibrous form, CSH II in a honeycomb-like structure called "honeycomb," CSH III forms isometric grains, and CSH IV forms spherical aggregates. The results of the research, obtained using qualitative-quantitative techniques such as X-ray diffraction (XRD) method, are presented in Tables 10, 11, and in Figure 6.

Analysis of the research results presented in tables 11 showed that the main hydration products

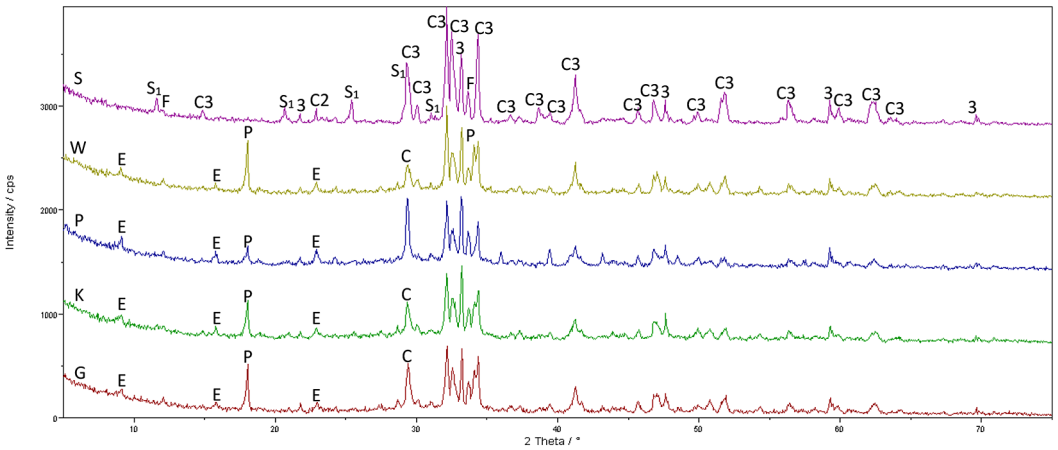

Figure 6. X-ray diffraction pattern of the sample with symbol marked with the symbol 6 of model cement. Description of crystal phases: 3- C_3A; F-ferrite; S_1 – calcium sulfate; E-ettringite; C2- C_2S; C3- C_3S; P – $Ca(OH)_2$; C – $CaCO_3$

Table 10. The degree of hydration in the sample model cement with symbol 6 expressed in wt%

Phases	Reaction degrees in %			
Sample designation	2W	2P	2K	2G
Reaction environment	Water	Chicken litter	Corn silage	Pig slurry
C_3S	56.8	65.6	54.5	71.5
β-C_2S	44.8	40.1	50.0	42.8
C_3A	100	100	100	100
C_4AF	9.0	2.5	14.2	12.8
Gypsum	100	100	100	100

Table 11. Quantitative analysis of phase hydration products in model cement sample 6 expressed in wt%

Newly formed phases	Content in % by weight phases resulting from reactions with aqueous solutions			
Sample designation	6W	6P	6K	6G
Reaction environment	Water	Chicken litter	Corn silage	Pig slurry
$Ca(OH)_2$	9.5	5.5	0	9.0
$CaCO_3$	3.5	10.0	6.3	6.0
Remaining phases and amorphous	The phases of weakly crystalline CSH compounds, hydroxy-AFm, hydrated calcium aluminates, ettringite, $C_4A\hat{C}H_{12}$ monocarboaluminate, $C_4A\hat{C}_{0.5}H_{12}$ hemicarboaluminate and amorphous iron hydroxides are visible in the background.			
	21.1	14.7	21.4	38.4
GOF	2.33	2.02	2.17	2.38
pH	12.52	11.15	7.56	6.98

of the synthetic cement samples "6" are phases $Ca(OH)_2$, $CaCO_3$, and amorphous CSH phases, along with residues of unreacted parts of starting phases. Additionally, low contents of poorly crystalline phases such as hydroxy-AFm, hydrated calcium aluminates, ettringite, monocarboaluminate $C_4A\hat{C}H_{12}$, hemicarboaluminate $C_4A\hat{C}_{0.5}H_{12}$, and amorphous iron hydroxides can be observed. Due to their low crystallinity level and difficulties in interpreting results caused by reflex coincidence, their content was included in the content of amorphous phases. Evaluation of the results presented in table 11 shows similarity in the levels and trends of degrees of reaction compared to pure phases C_3S, β-C_2S, and C_4AF after 10 months of hydration, whereas phases C_3A and gypsum reacted completely during this period. It was also confirmed that brownmillerite - C_4AF is the least reactive phase, resistant to the effects of biological corrosion, with the degree of reaction of this phase ranging from only 2.5% to about 14%, and the content of amorphous phases in the tested preparations ranged from 15% to 38%. It is worth noting the differences in the levels of degrees of reaction and content, both crystalline and newly formed phases, depending on the pH of the maturation environment of the preparations. Pellet samples, taken from their maturation environments, retained their original shape and were characterized by a lack of clear corrosion traces with high hardness. The high level of goodness-of-fit coefficients GOF in X-ray diffraction studies, ranging from 3.8 to 5.3, indicates the high reliability of the presented research results.

Results of the degree of reaction of model cement (symbol 8) with the addition of the γ-C_2S and $C_{12}A_7$ phase

It was decided that the mineral composition of the synthetic cement model (symbol 8) and γ-C_2S should approximately contain the following components: C_3S around 35%; β-C_2S around 16%; γ-C_2S+$C_{12}A_7$ (including 17.5% C_2S and 7.5% $C_{12}A_7$) totaling about 25%; C_3A about 2%; C_4AF about 9%, and about 6% gypsum. Synthetic calcium silicate γ-C_2S was obtained in larger quantities during research on self-disintegration processes of self-decomposing compacts, using the comprehensive method of Prof. J. Grzymek, simultaneously with obtaining aluminum hydroxide (oxide) and Portland cements. In our case, the preparation is characterized by the participation of approximately 30% by weight of the mayenite phase $C_{12}A_7$ in its synthesis process. This is a condition used in the method of J. Grzymek, which allows lowering the synthesis temperature and shortening the time, while ensuring the proper course of the self-decomposition process. The γ-calcium orthosilicate obtained in this way is almost inactive in hydration processes, characterized by a very high degree of comminution exceeding 10000 cm^2/g, which was determined by the Blaine method. A detailed description of the synthesis and self-decomposition process is available in the literature.

Analysis of the results of previous studies allows for a preliminary assessment of the usefulness of additives of the γ-C_2S phase together with the presence of the $C_{12}A_7$ phase to increase the resistance of mortars and concrete mixes to corrosion. It also appears that the close chemical composition relationship between the β-C_2S and γ-C_2S phases may additionally influence the course of hydration processes and increase the consistency of the investigated mixes.

The synthetic minerals were weighed and crushed in appropriate weight proportions, then mixed and homogenized for a period of 5 hours. As a result of these actions, an approximately three-kilogram sample of model cement named "8 + γ-C_2S" was obtained, whose mineral composition was determined by X-ray methods, presenting as follows (in % by weight): C_3S – 37.2%; β-C_2S – 17.8%; γ-C_2S – 19.0%; $C_{12}A_7$ – 8.1%; C_3A – 2.0%; C_4AF – 9.5%; Gypsum – 6.4%.

From the sample of model cement, preparations in the form of pellets were obtained, which were then placed in containers containing water and mixtures of water with biological additives. After 30 days of curing, the samples were dried, crushed, and subjected to further analysis. The results of these studies, obtained using the previously discussed qualitative-quantitative techniques, X-ray diffraction method, were presented in Tables 12 and 13, and in Figure 7.

The first significant conclusion drawn from the analysis of the obtained pH results of the solutions is the fact of minimal differences in their levels, ranging from 11.85 to 12.72. Such values exclude potential effects of the presence of "gram-negative" and "gram-positive" bacteria. Such uniformity is atypical for samples containing phases C_3S, β-C_2S, C_4AF, especially in the case of model cement (symbol 6). This is likely due to the addition of the γ-C_2S phase along with the presence of the $C_{12}A_7$ phase.

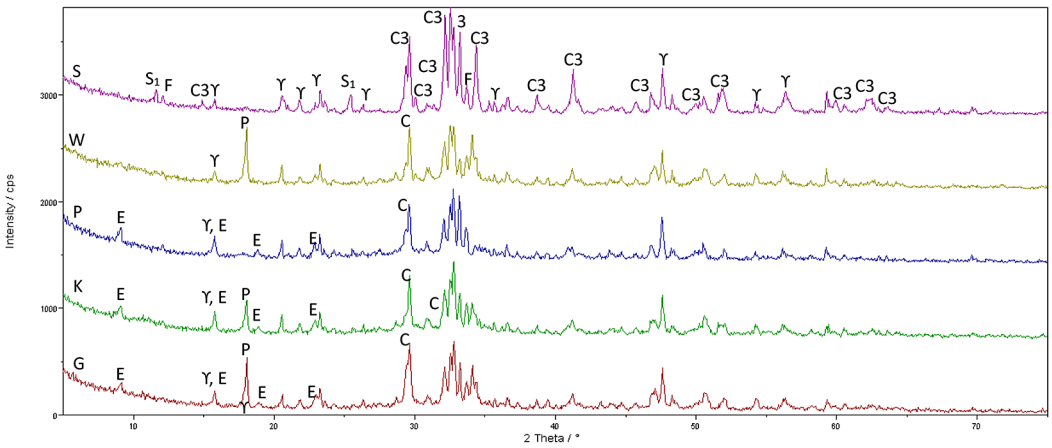

Figure 7. X-ray diffraction pattern of the sample marked with model cement symbol 8 with the addition of γ-C_2S and $C_{12}A_7$. Description of crystal phases: 3 – C_3A; F-ferrite; S_1 – calcium sulfate; E-ettringite; C2 – C_2S; C3 – C_3S; P – $Ca(OH)_2$; γ – γ-C_2S

Table 12. The degree of hydration in the sample model cement with symbol 8 with the addition γ-C_2S and $C_{12}A_7$ expressed in wt%

Phases	Reaction degrees in %			
Sample designation	8W	8P	8K	8G
Reaction environment	Water	Chicken litter	Corn silage	Pig slurry
C_3S	68.0	42.0	34.5	30.0
β-C_2S	28.0	36.5	41.5	32.5
γ-C_2S	10.5	14.0	15.5	9.0
C_3A	100.0	100.0	100.0	100.0
$C_{12}A_7$	100.0	100.0	100.0	100.0
C_4AF	5.0	0.0	13.0	11.0
Gypsum	100.0	100.0	100.0	100.0

Table 13. Quantitative analysis of phase hydration products in model cement sample 8 with the addition of γ-C_2S and $C_{12}A_7$ expressed in wt%

Newly formed phases	Content in % by weight phases resulting from reactions with aqueous solutions			
Sample designation	8W	8P	8K	8G
Reaction environment	Water	Chicken litter	Corn silage	Pig slurry
$Ca(OH)_2$	12.5	0.0	4.5	6.5
$CaCO_3$	8.0	11.0	12.0	11.0
Ettryngite	5.0	8.5	9.0	11.0
Remaining phases and amorphous	Phases of weakly crystalline CSH compounds, hydrated calcium aluminates, ettringite, hydroxy-AFm, monocarboaluminate $C_4A\hat{C}H_{12}$, hemicarboaluminate $C_4A\hat{C}_{0.5}H_{12}$ and amorphous iron hydroxides visible in the background.			
	37	51	45	43
GOF	2.184	2.636	2.625	2.290
pH	12.72	11.95	11.86	12.21

The observed high pH levels, especially for the model cement with the addition of γ-C_2S and $C_{12}A_7$, exclude the presence of live bacterial organisms and their potential corrosive actions.

Interesting results concern the sample of cement (symbol 8) hydrating in a water solution of pomace, where there is no reaction of the C_4AF phase and no presence of the $Ca(OH)_2$ phase

observed. It is noteworthy the high level of calcium carbonate content in all hydrating preparations in the tested environments. It is also worth considering the possibility of the presence of other crystalline forms of calcium carbonate and its presence in the form of poorly crystalline phase. The results of the degree of reaction analysis of the γ-C_2S phase show the lowest level in the case of cement 8. Probably, the weak hydraulic activity of the γ-C_2S phase affects the relatively low content of amorphous phases, considering the presence of the planned special additive. The presence of ettringite phase is associated with complete reaction of the C_3A, $C_{12}A_7$, and gypsum phases.

In summary, X-ray analysis reveals crystalline or amorphous phases listed in table 12, in the "remaining phases" section, suggesting the possibility of phase diversity in the tested samples. [Pyzalski et al., 2023; Durczak et al., 2023].

Biological studies of the reaction environment

Biological studies of suspensions in contact with phases C_3S, β-C_2S (1); C_4AF (2), as well as with model cements (6 and 8), were initially conducted by directly measuring their pH and performing bacterial cultures on agar (PCA, plate count agar, Biomaxima) under standard incubation conditions (37 °C/24h). In the second part of the study, agar surfaces were examined for the presence of bacteria after 24 hours of incubation. Swabs were taken from materials showing a positive bacterial response and stained using the Gram method (showing the presence of Gram-negative and Gram-positive bacteria). Subsequently, to obtain microscopic images, cultures obtained from agar cultures were stained with crystal violet and safranin to determine the presence of "Gram-negative" and "Gram-positive" bacteria. The obtained results were presented in the form of microscopic images of preparations and photographs of the preparations themselves (Fig. 8–10). The pH results of the suspensions are presented in Table 14. The obtained results of the bacterial cultures correlate with the pH data. Where the pH was around neutral or slightly acidic values, bacterial growth after 24 hours of incubation was visible in the macroscopic images obtained (Fig. 8–10).

The obtained microscopic images of all examined specimens, in which the presence of Gram-negative and Gram-positive bacteria was detected, were analyzed. Staining with crystal violet and fuchsin was performed on agar cultures obtained from suspensions P, G, and K, as well as 1G, 6G, 2K, and 6K, to determine the presence of Gram-negative and Gram-positive bacteria. The resulting microscopic images are presented in Figure 12.

Table 14. Results of pH tests for suspensions of aqueous solutions of biological media

Sample W	pH	Sample G	pH	Sample K	pH	Sample P	pH
H_2O	7.61	G	4.65	K	6.88	P	6.41
1W	12.81	1G	6.87	1K	10.21	1P	10.64
2W	12.32	2G	7.12	2K	9.06	2P	10.85
6W	12.52	6G	6.98	6K	7.56	6P	11.15
8W	12.72	8G	12.21	8K	11.86	8P	11.95

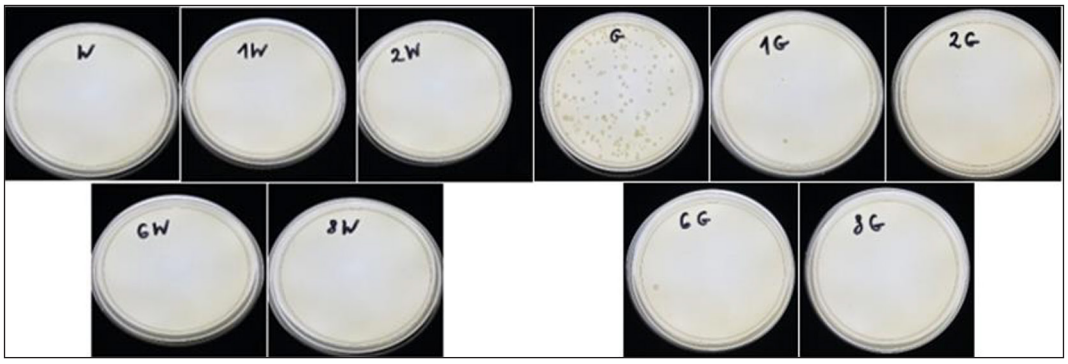

Figure 8. Bacterial culture for suspensions marked with the symbol W and G after 24 hours of culture

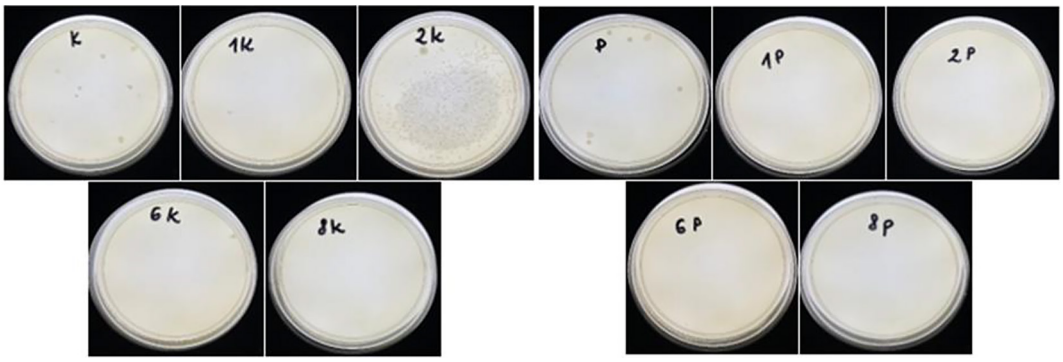

Figure 9. Bacterial culture for suspensions marked with the symbol K and P after 24 hours of culture

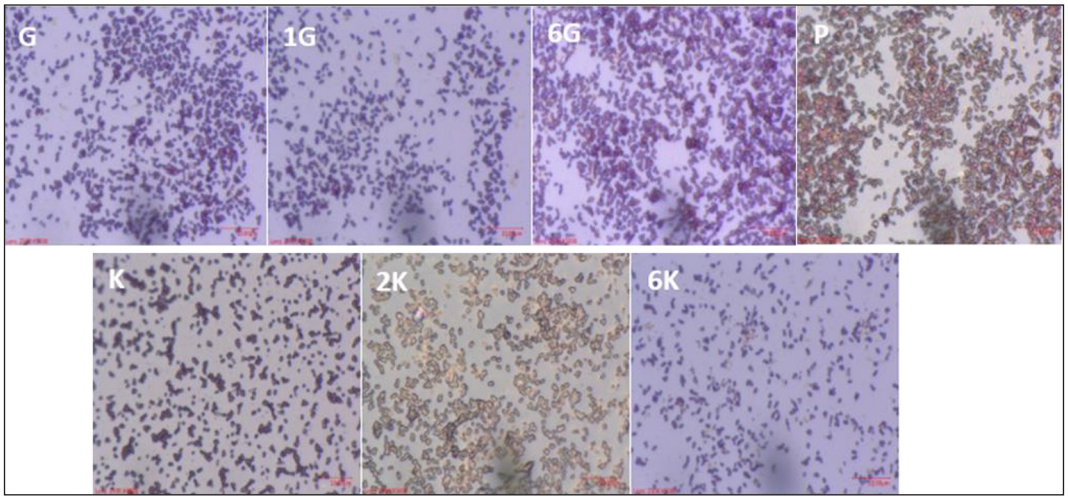

Figure 10. Bacterial inoculation for suspensions marked with the symbol G, P, K after 24 hours of culture

The execution of this type of research aimed at finding answers to intriguing and original questions concerning the assessment of the existence and lifespan of bacteria over a period of 30 days in the presence of water environments and environments strongly dependent on pH in biological suspensions. The obtained results demonstrate the influence of environmental pH on the presence of bacteria and their lifespan. It was found that in cases where the pH exceeds 9, the preparations do not contain any living bacterial organisms, whereas in acidic pH (~ pH 4) and neutral (pH 6–7) environments, both "Gram-negative" and "Gram-positive" bacteria are present in suspensions. It can be assumed that a pH level above 9 in the sample storage environment leads to relatively rapid bacterial death. Taking into account the relationship between the presence of bacteria and the pH of the environment, in the subsequent part of the study, efforts were made to organize the results of the remaining research according to the decreasing order of the pH values, ranging from approximately 12.72 to 4.65. To confirm the above conclusions, microscopic images documenting the presence of bacteria in aqueous environments with pH values lower than 9 were additionally included and labeled as follows: G, 1G, 6G, K, 2K, 6K, and P. The originality of the results presented above lies in the fact that despite diligent efforts, it was not possible to compare them with other scientific and published studies [Bagga et al., 2023; Ying et al., 2024].

Summary

The experimental work focused on investigating the influence of aqueous solutions of manure, slurry, and silage on the hydration processes of individual clinker minerals such as; C_3S (allite), β-C_2S (belite), C_3A, and C_4AF (brownmillerite). The primary objectives of these studies were to determine the degree of advancement of hydration reactions, qualitative and quantitative analysis of newly formed hydration products, and to

assess the impact of biological corrosion in various cementitious mixes. The hydration processes of the silicate minerals C_3S and β-C_2S proceeded with the precipitation of phases such as $Ca(OH)_2$, $CaCO_3$ along with various weakly crystalline C-S-H phases, which were also contaminated with elements Mg, S, P, Ti, K, and Cl present in the aqueous solutions of biological media. Besides the above-mentioned phases, amorphous hydration products of synthetic clinkers were also observed. It was also noted that in cases involving biological additives, phases such as $Ca(OH)_2$ and $CaCO_3$ could occur in amorphous form, with the latter also occurring in its polymorphic forms such as aragonite and vaterite. During the course of the study, it was found that the phase C_3A, forming various types of defective, easily soluble, hydrated calcium aluminates, was the least resistant to the effects of biological corrosion. Undoubtedly, the presence of this mineral in cement reacting with aqueous waste solutions is undesirable and poses a fundamental threat to the durability of mixes and concretes. Calcium ferrite (C_4AF) proved to be the most resistant to the influences of biological factors among all the minerals examined. The results of the hydration studies showed the highest hardness among all macroscopically examined clinker minerals.

In addition to the aforementioned assumptions, research was also conducted on samples of model cement (composed of synthetic clinker minerals) with the following mineral composition: C_3S – 49.5%, β-C_2S – 24.7%, C_3A – 7.8%, C_4AF – 10.0%, Gypsum – 8.0%. The results of the studies allowed for finding answers to questions regarding the assessment of the existence and lifespan of bacteria in the presence of the aforementioned model cement over a period of 30 days, in an aqueous environment and in aqueous solutions with varying pH strongly dependent on the applied biological suspensions. The obtained results demonstrate the influence of the environmental pH on the presence of bacteria and their lifespan. It was found that at a pH value of 9, the samples did not contain any living bacterial organisms; however, at acidic pH (~ pH 4) and neutral (pH 6–7) environments, both "gram-negative" and "gram-positive" bacteria were present in suspensions. A pH value above 9 leads to relatively rapid bacterial death and thus likely inhibits biocorrosion processes. The analysis of the results of the corrosion of the model cement confirmed a significant similarity with the results obtained for individual cement minerals. The evaluation of the obtained results confirms that the pH level of the used solutions had a significant influence on the degree of changes in the phase composition of the samples, and consequently on the presence or lack of active biological matter producing, alongside biogas, carbon dioxide responsible for additional and strong carbonation effects. Based on the results of the aforementioned stages and the conducted research on the processes and properties of the γ-C_2S phase, it was concluded that despite its lack of hydraulic activity, this compound exhibits interesting anti-corrosive properties, particularly in the presence of the $C_{12}A_7$ phase. Subsequently, further research was conducted on the impact of biological factors on the physicochemical properties of model cement with the addition of the γ-C_2S phase. The initial mineral composition of the synthetic cement was as follows: C_3S – 35%; β-C_2S – 16%; γ-C_2S + $C_{12}A_7$ (including 17.5% C_2S and 7.5% $C_{12}A_7$); C_3A – 2%; C_4AF – 9%; and approximately 6% gypsum. The addition of approximately 18% γ-C_2S, including 7% mayenite, was specially designed as a reinforcing additive to enhance the anti-corrosive properties of Portland cement binders. Calcium orthosilicate was obtained through a special technology involving controlled synthesis and cooling of self-disintegrating clinker, resulting in a finely grained powder with a specific surface area of approximately 10,000 cm²/g and an average grain size below 15 μm.

It was observed that in the case of all cement preparations with the addition of the γ-C_2S and $C_{12}A_7$ phases, the aqueous solutions, along with additives, exhibited a pH level ≥ 11.86, thus excluding the presence of active bacteria. It should be emphasized the uniformity and complete sealing of the microstructure of the sample fractures associated with the presence of the γ-C_2S and $C_{12}A_7$ additives (Kluska et al. 2003). The applied additive acts as a protective barrier between the corrosive environment and the cement matrix. Additionally, the presence of phases formed during the hydration process – most likely amorphous calcium hydroxide and carbonate compounds, along with crystals resembling C-S-H morphology – was detected. Atomic analysis results ruled out the possibility of identifying this phase as a hydrated calcium silicate variety. The presence of the $Ca(OH)_2$ phase was also noted, which differed drastically from the morphology of known calcium hydroxide forms. SEM analyses of hydrated synthetic cement preparations with the addition

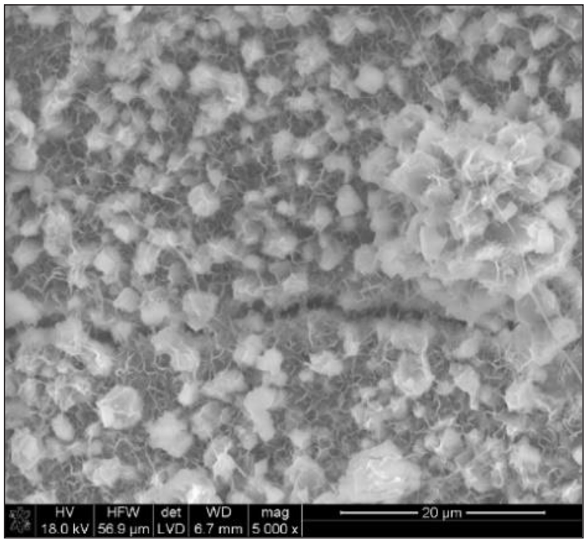

Figure 11. Microstructure of cement paste with the addition of $C_{12}A_7$ and γ-C_2S

of γ-C_2S and $C_{12}A_7$ always revealed a nearly uniform surface of the fracture preparations, regularly filled with white reaction products. Few larger clusters of hydrates and calcium orthosilicate grains were also observed in the samples.

The bound cement preparations, in all examined corrosive media, exhibited the highest hardness. The microstructure of the sample revealed its exceptional density, where all spaces were fully occupied by hydration products of $C_{12}A_7$ and γ-C_2S (Fig. 11). Such a model of cement matrix construction prevents and limits the penetration of the corrosive agent into the sample interior. In summary, it can be concluded that the cycle of publications resulting from a series of research works represents a scientific achievement and contributes to the development of the environmental engineering discipline, particularly regarding research on the impact of biological aggression on the composition of synthetic clinker minerals and phases of cementitious and model cement systems. Simultaneously, the understanding of the possibilities of obtaining and modeling the properties of the γ-C_2S and $C_{12}A_7$ phases has enabled the determination of the appropriate additive to enhance the resistance of cementitious materials used in the construction of potential bioreactors against biological corrosion. This finely ground additive, thoroughly homogenized with Portland cement, allows for the achievement of high density during hydration processes, thereby blocking potential progress of biological corrosion while increasing the strength of the bound material.

In addition to issues related to the addition of the γ-C_2S phase, efforts have been made to further enhance the corrosion resistance of cementitious materials by using additives of specified phases of aluminates and calcium ferrites. Since both of the additives used and investigated represent, in a sense, an extension of the typical mineral composition of Portland cements, it is certainly possible to combine their use, which will be the subject of further research.

CONCLUSIONS

Based on the presented results of phase composition analysis and thermal analysis of cement pastes, as well as the conducted research on the influence of aqueous solutions such as manure, slurry, and silage on the hydration processes of individual clinker minerals and the properties of model cement, the following conclusions can be drawn:

1. Presence of amorphous phase: The elevation of the background in the range of 25–40 degrees 2Θ suggests the presence of an amorphous phase in the samples. This is significant as it indicates the possibility of biological corrosion, but also reactions between cement components such as calcium hydroxide and carbon dioxide, released during oxygen-deprived respiration by bacteria.
2. Changes in phase composition: Observed changes in the intensity of diffraction reflexes indicate changes in the mass ratio of portlandite to calcite, confirming the variable impact of biological corrosion processes on the phase composition of cement samples.
3. Impact of biological corrosion on strength: Samples subjected to biological corrosion showed reduced compressive strength compared to control samples stored in water. This suggests that biological aggression can lead to the destruction of the cement sample structure, which may negatively affect their mechanical parameters.
4. Changes in sample structure: Infrared spectroscopy analysis showed changes in the structure of cement pastes subjected to biological corrosion, which may result from the formation or breaking of hydrogen bonds, leading to degradation of the cement matrix.
5. Increase in calcium carbonate content: The presence of increased calcium carbonate content in samples subjected to biological corrosion may lead to sealing of surface pores of the samples but may also affect the reduction of their strength parameters.

6. It was found that the presence of different types of biological solutions affects the hydration process of clinker minerals, leading to the formation of phases such as $Ca(OH)_2$, $CaCO_3$, and weakly crystalline C-S-H phases. Additionally, contamination with elements present in the solutions was observed, which may influence the properties of the final hydration products.
7. The C_3A phase proved to be the least resistant to biological factors, posing a threat to the durability of pastes and concretes. Meanwhile, the C_4AF phase showed the highest resistance to biological influences, confirming its importance in ensuring the durability of cement structures.
8. Research has shown that the pH of the environment has a significant impact on the presence of bacteria. A pH value above 9 results in the inhibition of biocorrosion processes, which may be crucial for ensuring the durability of cement structures.
9. Addition of γ-C_2S and $C_{12}A_7$ phases proved to be an effective way to improve the resistance of cement to biological corrosion. Additionally, the microstructure of cement with these additives exhibited high density, limiting the penetration of corrosive agents.
10. The research results open perspectives for further work on optimizing the composition of cement to increase its resistance to biological factors. The use of anti-corrosion additives such as γ-C_2S and $C_{12}A_7$ phases, as well as experiments with other phases of aluminates and calcium ferrites, may lead to further improvements in the durability of cement structures.

In summary, the research results indicate a comprehensive impact of biological corrosion on the phase composition, structure, and mechanical parameters of cement pastes. This is important for assessing the durability and stability of structures, especially in the context of their exposure to environments containing organic matter.

Acknowledgements

The author wishes to thank President of DSI Schaum Chemie, a Sandvik Company, Engineer Henryk Kuźma, for the generous financial support of the presented research work. Sir, your involvement has been and remains crucial in achieving our common goals and opening the door to future cooperation in the industrial application of the research presented. I am immensely grateful for your trust and willingness to collaborate. I am also convinced that our synergy will yield fruitful results, beneficial for both parties and for the sustainable eco-energy economy.

REFERENCES

1. Bagga M., Justo-Reinoso I., Hamley-Bennett Ch., Merces G., Luli S., Therese Akono A., Masoero E., Paine K., Gebhard S., Ofiteru I. D., 2023. Assessing the potential application of bacteria-based self-healing cementitious materials for enhancing durability of wastewater treatment infrastructure, Cement and Concrete Composites 143. https://doi.org/10.1016/j.cemconcomp.2018.08.007
2. Baroghel-Bouny V., Capra B., Laurens D., 2008. La durabilité des armatures et du béton d'enrobage, Durabilité Bétons, Presse de l'ENCP, 303–385.
3. Bertron A., 2014. Understanding interactions between cementitious materials and microorganisms: a key to sustainable and safe concrete structures in various contexts, Mater. Struct. 47 1787–1806, https://doi.org/10.1617/s11527-014-0433-1
4. Bertron A., Duchesne J., 2013. Attack of Cementitious Materials by Organic Acids in Agricultural and Agrofood Effluents, Perform. Cem.-Based Mater. Aggress. Aqueous Environ, Springer, Dordrecht, 31–173, https://doi.org/10.1007/978-94-007-5413-3_6
5. Bertron A., Peyre-Lavigne M., Patapy C., Erable B., 2017. Biodeterioration of concrete in agricultural, agro-food and biogas plants: state of the art and challenges, RILEM Tech. Lett. 2, 83–89, https://doi.org/10.21809/rilemtechlett.2017.42
6. Carde C., Escadeillas G., R. François, 1997. Use of ammonium nitrate solution to simulate and accelerate the leaching of cement pastes due to deionized water, Mag. Concr. Res. 49, 295–301.
7. Cole S., Frank J.R., 1988. Methane from Biomass: A Systems Approach, Springer, Netherlands.
8. Durczak K., Pyzalski M., Brylewski T., Sujak A., 2023. Effect of Variable Synthesis Conditions on the Formation of Ye'elimite-Aluminate-Calcium (YAC) Cement and Its Hydration in the Presence of Portland Cement (OPC) and Several Accessory Additives. Materials, 16, 6052. https://doi.org/10.3390/ma16176052
9. Durczak K., Pyzalski M., Pilarski K., Brylewski T., Sujak A., 2021.The Effect of Liquid Slurry-Enhanced Corrosion on the Phase Composition of Selected Portland Cement Pastes. Materials 14, 1707. https://doi.org/10.3390/ma14071707
10. Escadeillas G., 2013. Ammonium Nitrate Attack on Cementitious Materials,

Perform. Cem.-Based Mater. Aggress. Aqueous Environ, Springer, Dordrecht, 113–130, https://doi.org/10.1007/978-94-007-5413-3_5

11. Escadeillas G., Hornain H., 2008. La durabilité des bétons vis-à-vis des environnements chimiquement agressifs, Durabilité Bétons, Presse de l'ENCP, 613–705.
12. Evans G.M., Furlong J.C., 2003. Environmental Biotechnology - Theory and Application, John Wiley & Sons.
13. Fehrenbach H., Giegrich J., Reinhardt G., Sayer U., Gretz M., Lanje K., Schmitz J., 2008. Kriterien einer nachhaltigen Bioenergienutzung im globalen Ma\s sstab, UBA-Forschungsbericht, 206,41–112.
14. Gerardi M.H., 2003.The Microbiology of Anaerobic Digesters, John Wiley & Sons.
15. Kayhanian M.,1999. Ammonia inhibition in high-solids biogasification: an overview and practical solutions, Environ. Technol. 20, 355–365, https://doi.org/10. 1080/09593332008616828
16. Kluska S., Jonas S., Walasek E., Stapinski T., Pyzalski M., 2003. Influence of SiC infiltration of some properties of porous carbon materials. Journal of the European Ceramic Society, 23, 1509-1515.
17. Koenig A., Dehn F., 2016. Biogenic acid attack on concretes in biogas plants, Biosyst. Eng. 147, 226–237, https://doi.org/10.1016/j.biosystemseng.2016.03.007
18. Koenig A., Dehn F., 2016. Main considerations for the determination and evaluation of the acid resistance of cementitious materials, Mater. Struct. 49, 1693–1703, https://doi.org/10.1617/s11527-015-0605-7
19. Koenig A., Herrmann A., Overmann S., Dehn F., 2017. Resistance of alkali-activated binders to organic acid attack: assessment of evaluation criteria and damage mechanisms, Constr. Build. Mater. 151, 405–413, https://doi.org/10.1016/j.conbuildmat.2017.06.117
20. Kothari R., Pandey A.K., Kumar S., Tyagi V.V., Tyagi S.K., 2014. Different aspects of dry anaerobic digestion for bio-energy: an overview, Renew. Sust. Energ. Rev. 39 174–195, https://doi.org/10.1016/j.rser.2014.07.011
21. Lea F.M., The action of ammonium salts on concrete, 1965. Mag. Concr. Res. 52, 115–116 https://doi.org/10.1680/macr.1965.17.52.115
22. Li Y., Park S.Y., Zhu J., 2011. Solid-state anaerobic digestion for methane production from organic waste, Renew. Sust. Energ. Rev. 15, 821–826, https://doi.org/10.1016/j.rser.2010.07.042
23. Magniont C., Coutand M., Bertron A., Cameleyre X., Lafforgue C., Beaufort S., Escadeillas G., 2011. A new test method to assess the bacterial deterioration of cementitious materials, Cem. Concr. Res. 41, 429–438, https://doi.org/10.1016/j. cemconres.2011.01.014
24. Morandeau A., Thiéry M., Dangla P., 2014. Investigation of the carbonation mechanism of CH and C-S-H in terms of kinetics, microstructure changes and moisture properties, Cem. Concr. Res. 56 153–170, https://doi.org/10.1016/j.cemconres.2013.11.015
25. PN-EN 196-1:2016-07, 2018. Cement—Part 1. Cement Test Methods—Part 1: Determination of Strength. Polish Committee for Standardization: Warsaw, Poland.
26. Pyzalski M., Brylewski T., Sujak A., Durczak K., 2023. Changes in the Phase Composition of Calcium Aluminoferrites Based on the Synthesis Condition and Al_2O_3/Fe_2O_3 Molar Ratio. Materials 16, 4234. https://doi.org/10.3390/ma16124234
27. Pyzalski M., Dabek J., Adamczyk A., Brylewski T., 2021. Physicochemical Study of the Self-Disintegration of Calcium Orthosilicate in the Presence of the C12A7 Aluminate Phase. Materials 14, 6459. https:// doi.org/10.3390/ma14216459
28. Pyzalski M., Sujak A., Durczak K., Murzyn P., Brylewski T., Sitarz M., 2023. The Effect of Biological Corrosion on the Hydration Processes of Synthetic Tricalcium Aluminate (C3A). Materials, 16, 2225. https://doi.org/10.3390/ma16062225
29. Sujak A., Pyzalski M., Durczak K., Brylewski T., Murzyn P., Pilarski K., 2022. Studies on Cement Pastes Exposed to Water and Solutions of Biological Waste. Materials, 15, 1931. https:// doi.org/10.3390/ma15051931
30. Thiery M., 2005. Modélisation de la carbonatation atmosphérique des matériaux cimentaires: Prise en compte des effets cinétiques et des modifications microstructurales et hydriques, Ecole Nationale des Ponts et Chaussées.
31. Voegel C., Bertron A., Erable B., 2016. Mechanisms of cementitious material deterioration in biogas digester, Sci. Total Environ. 571, https://doi.org/10.1016/j.scitotenv.2016.07.072
32. Voegel C., Durban N., Bertron A., Landon Y., Erable B., 2019. Evaluation of microbial proliferation on cementitious materials exposed to biogas systems, Environ. Technol. 1–11, https://doi.org/10.1080/09593330.2019.1567610
33. Ying W., Ye H., 2024. Evaluation of novel copper-based antimicrobial admixtures for biocorrosion mitigation of cement paste. Cement and Concrete Composites 150. https://doi.org/10.1016/j.cemconcomp.2024.105536